Structure
Article

Hierarchical Binding of Cofactors to the AAA ATPase p97

Petra Hänzelmann,[1,*] Alexander Buchberger,[2] and Hermann Schindelin[1,*]
[1]Rudolf Virchow Center for Experimental Biomedicine, University of Würzburg, Josef-Schneider-Str. 2, 97080 Würzburg, Germany
[2]Department of Biochemistry, Biocenter, University of Würzburg, Am Hubland, 97074 Würzburg, Germany
*Correspondence: petra.haenzelmann@virchow.uni-wuerzburg.de (P.H.), hermann.schindelin@virchow.uni-wuerzburg.de (H.S.)
DOI 10.1016/j.str.2011.03.018

SUMMARY

The hexameric AAA ATPase p97 is involved in several human proteinopathies and mediates ubiquitin-dependent protein degradation among other essential cellular processes. Via its N-terminal domain (N domain), p97 interacts with multiple regulatory cofactors including the UFD1/NPL4 heterodimer and members of the "ubiquitin regulatory X" (UBX) domain protein family; however, the principles governing cofactor selectivity remain to be deciphered. Our crystal structure of the FAS-associated factor 1 (FAF1)UBX domain in complex with the p97N domain reveals that the signature Phe-Pro-Arg motif known to be crucial for interactions of UBX domains with p97 adopts a *cis*-proline configuration, in contrast to a *cis-trans* mixture we derive for the isolated FAF1UBX domain. Biochemical studies confirm that binding critically depends on a proline at this position. Furthermore, we observe that the UBX proteins FAF1 and UBXD7 only bind to p97-UFD1/NPL4, but not free p97, thus demonstrating for the first time a hierarchy in p97-cofactor interactions.

INTRODUCTION

The hexameric AAA ATPase (*A*TPase *a*ssociated with various *a*ctivities) p97, also referred to as valosin-containing protein (VCP), participates in a large variety of cellular processes including protein quality and cell cycle control, membrane fusion, transcriptional activation, DNA-damage repair, apoptosis, and autophagy (Halawani and Latterich, 2006; Schuberth and Buchberger, 2008; Vij, 2008; Ye, 2006). p97 plays a central role in the ubiquitin proteasome system (UPS), for instance in the endoplasmic reticulum-associated degradation (ERAD) pathway, where it catalyzes the ATP-driven extraction of misfolded proteins from the ER back into the cytoplasm, and serves as a molecular chaperone, guiding ubiquitylated substrates to the 26S proteasome for degradation (Hirsch et al., 2009).

p97 mediates these diverse cellular processes with the help of various adaptor proteins that specifically recruit ubiquitylated substrates (Yeung et al., 2008). This enzyme is composed (DeLaBarre and Brunger, 2003; Zhang et al., 2000) of two ATPase domains (D1 and D2) and an N-terminal domain (N domain) to which most adaptor proteins bind. The two best-characterized adaptors of p97 are p47 and the UFD1/NPL4 heterodimer, which bind to the N domain in a mutually exclusive manner (Bruderer et al., 2004; Meyer et al., 2000) and target p97 to membrane fusion events and the ERAD pathway, respectively. Both complexes differ significantly in stoichiometry and symmetry, reflecting their specific actions and ability to interact with additional adaptors that cooperate with p97 in diverse cellular pathways (Dreveny et al., 2004; Pye et al., 2007).

Proteins that contain the so-called ubiquitin regulatory X (UBX) domain, which features a ubiquitin-like fold, constitute the largest family of p97 adaptor proteins and bind to the N domain through a highly conserved R…FPR motif of exposed side chains (Buchberger et al., 2001; Dreveny et al., 2004; Schuberth and Buchberger, 2008). In humans, 13 members have been identified that can be divided into two major subclasses based on their ability to bind ubiquitylated substrates (Alexandru et al., 2008; Schuberth and Buchberger, 2008): (i) UBX-only proteins (p37, ASPL, UBXD1 to UBXD6); and (ii) UBA-UBX proteins (p47, FAF1, SAKS1, UBXD7, UBXD8). The second group contains an N-terminal ubiquitin-associated (UBA) domain involved in substrate binding, and a C-terminal UBX domain mediating interactions with p97. These proteins also associate with a large number of ubiquitin ligases. However, not all UBX proteins interact with p97 through their UBX domain. For example the UBX-only protein UBXD1 that lacks the conserved FPR signature instead utilizes a so-called bipartite-binding mechanism in which two separate regions of UBXD1 interact with p97, in this case with its N domain and its C terminus (Kern et al., 2009).

In the ERAD pathway UBX proteins are involved in the retro-translocation of misfolded proteins into the cytoplasm by recruiting p97 to the ER membrane as well as in the targeting of polyubiquitylated substrates to p97 and the proteasome. FAF1 (FAS-associated factor 1), a UBA-UBX protein composed of multiple protein-interacting domains, has been implicated as a tumor suppressor that is involved in the regulation of apoptosis and NF-κB activity, as well as in ubiquitylation and proteasomal degradation (Menges et al., 2009). UBXD7, another UBA-UBX protein, has been shown to link p97 to the ubiquitin ligase CUL2/VHL and its substrate hypoxia-inducible factor 1α (HIF1α) (Alexandru et al., 2008).

p97 itself has been implicated in cancer and a wide variety of neurodegenerative disorders, including Parkinson's disease, Lewy body disease, Huntington's disease, and spinocerebellar ataxia type III (SCAIII; Machado-Joseph disease) (Haines, 2010). Mutations in p97 cause inclusion body myopathy, Paget's disease of the bone, and frontotemporal dementia (IBMPFD),

Table 1. Data Collection and Refinement Statistics

	p97N	FAF1UBX	p97N-FAF1UBX
Data Collection			
Wavelength (Å)	0.9184	0.9792	0.9184
Space group	$P3_1$	$P6_1$	$P6_5$
Cell dimensions			
a = *b*, *c* (Å)	60.1, 63.1	92.6, 108.5	88.1, 66.9
α = β, γ (°)	90,120	90,120	90, 120
Resolution (Å)[a]	40.34–2.65 (2.79–2.65)	80.34–3.0 (3.16–3.0)	38.14–2.0 (2.11–2.0)
$\langle I/\sigma(I)\rangle$[a,b]	16.4 (2.7)	12.5 (2.9)	16.5 (3.9)
Completeness (%)[a]	100 (100)	100 (100)	98.5 (97.8)
Redundancy[a]	4.5 (4.5)	5.2 (3.6)	7.7 (7.7)
R_{sym}[a,c]	5.0 (57.3)	9.5 (51.8)	7.7 (53.4)
Refinement			
Resolution (Å)	30.28–2.65	42.65–3.0	33.14–2.0
Number of reflections	7,267	10,401	19,395
R_{cryst}/R_{free}[d]	19.5/23.6	17.8/25.8	16.9/21.0
Number of atoms			
Protein	1,346	2,767	2,114
Ligands	16	15	1
Water	16	24	146
Rmsd			
Bond lengths (Å)	0.012	0.009	0.007
Bond angles (°)	1.351	1.324	1.103
Estimated coordinate error (Å)[e]	0.43	0.43	0.21
B factors (Å^2)			
Protein (p97N/UBX)	76.8/–	–/54.1	34.7/44.7
Water	65.4	43.9	41.1
Ramachandran statistics[f]			
Favored (%)	94.0	93.2	96.6
Allowed (%)	3.0	4.9	3.4
Outliers (%)	3.0	1.9	0

[a] Numbers in parentheses refer to the respective highest resolution data shell in each data set.

[b] $\langle I/\sigma I\rangle$ indicates the average of the intensity divided by its average standard deviation.

[c] $R_{sym} = \Sigma_{hkl}\Sigma_i|I_i - \langle I\rangle|/\Sigma_{hkl}\Sigma_i\langle I\rangle$, where I_i is the i^{th} measurement, and $\langle I\rangle$ is the weighted mean of all measurements of I.

[d] $R_{cryst} = \Sigma||F_o| - |F_c||/\Sigma|F_o|$, where F_o and F_c are the observed and calculated structure factor amplitudes. R_{free} is the same as R_{cryst} for 5% of the data randomly omitted from the refinement.

[e] Estimated coordinate error based on R_{free}.

[f] Ramachandran statistics indicate the fraction of residues in the favored (98%), allowed (>99.8%), and disallowed regions of the Ramachandran diagram, as defined by MolProbity (Davis et al., 2007).

a rare proteinopathy that mainly affects skeletal muscle, brain, and bone (Ju and Weihl, 2010). Mutations in p97 also cause autosomal-dominantly inherited amyotrophic lateral sclerosis (ALS), a fatal neurodegenerative disease characterized by motor neuron degeneration (Johnson et al., 2010).

In order to understand the mechanism underlying p97 cofactor selectivity and its role in ubiquitin-dependent protein degradation, we have characterized the interaction between UBA-UBX containing cofactors and p97. The crystal structure of p97N in complex with FAF1UBX as well as a detailed biochemical analysis of the p97-binding site revealed a conserved binding mode of the UBX R…FPR signature to the hydrophobic cleft formed between the two p97N subdomains. Biochemical studies demonstrate that FAF1 and UBXD7 only bind to p97-UFD1/NPL4, but not to free p97, thus demonstrating for the first time a hierarchy in p97-cofactor interactions.

RESULTS

FAF1UBX Binds into the p97N Domain Hydrophobic Interdomain Cleft

To obtain molecular details of the p97-FAF1 interaction, we solved the crystal structures of the p97N domain in complex with the FAF1UBX domain and in the free state. The apo form of the N domain was solved by molecular replacement with the N domain of the p97ND1 crystal structure as search model (PDB entry 1S3S) and was refined at 2.65 Å resolution to a crystallographic R factor of 19.5% and a free R factor of 23.6% (Table 1). The p97N-FAF1UBX complex was also solved by molecular replacement with the same search model for the N domain and the NMR structure of the FAF1UBX domain (Model 1 of PDB entry 1H8C) and was refined at 2.0 Å resolution to a crystallographic R factor of 16.9% and a free R factor of 21.0% (Table 1). As described earlier (DeLaBarre and Brunger, 2003; Zhang et al., 2000), the p97N domain (residues 10–186) contains two subdomains linked by a flexible linker of six amino acids: an N-terminal double ψ β-barrel (referred to as either Nn or Na); and a C-terminal α+β domain (Nc or Nb) with a central four-stranded antiparallel β sheet (Figure 1A). The FAF1UBX domain encompasses residues 570–649 and adopts the β-grasp (β-β-α-β-β-α-β) or ubiquitin-like fold, which is characterized by a five-stranded antiparallel β sheet (Figure 1A), a single helix on top of the β sheet, and a short 3_{10} helix inserted between β strands 4 and 5 (Buchberger et al., 2001).

The p97N-FAF1UBX interface is predominantly polar with 29% charged and 46% polar residues and only 25% nonpolar residues. The most critical interaction is located in the UBX loop region between β strands 3 and 4, the S3/S4 loop with the sequence ^{618}TFPR^{621}, that is an essential part of the conserved UBX ^{579}R…^{619}FPR^{621} signature motif. The aromatic side chain of Phe619 of the UBX domain inserts into a hydrophobic cleft created between the two N-terminal subdomains of p97 (Figure 1B). Val38, Phe52, Ile70, Leu72, Tyr110, and Tyr143 create this binding pocket and are involved in several hydrophobic interactions with UBX Leu616, Phe619, and Phe645 (Figure 1C). This pocket is restricted at its base by a salt bridge formed between Arg144 and Asp35 (NH2-OD2 3.2 Å and NH1-OD1 2.9 Å) that connects the Nn and Nc subdomains. In addition to these hydrophobic contacts, several main chain-side chain and side chain-side chain hydrogen bonds are observed, including Arg621 of FAF1 and Arg53 of p97 (Figure 1C). Arg53 also forms a hydrogen bond with the carbonyl oxygen of Phe619, which apparently stabilizes the S3/S4 loop conformation. UBX Arg579, the first arginine of the conserved UBX ^{579}R…^{619}FPR^{621} signature motif, is deeply buried in p97N and is 3.8 Å from the carbonyl oxygen of Val108, which is classified as a hydrogen bond despite

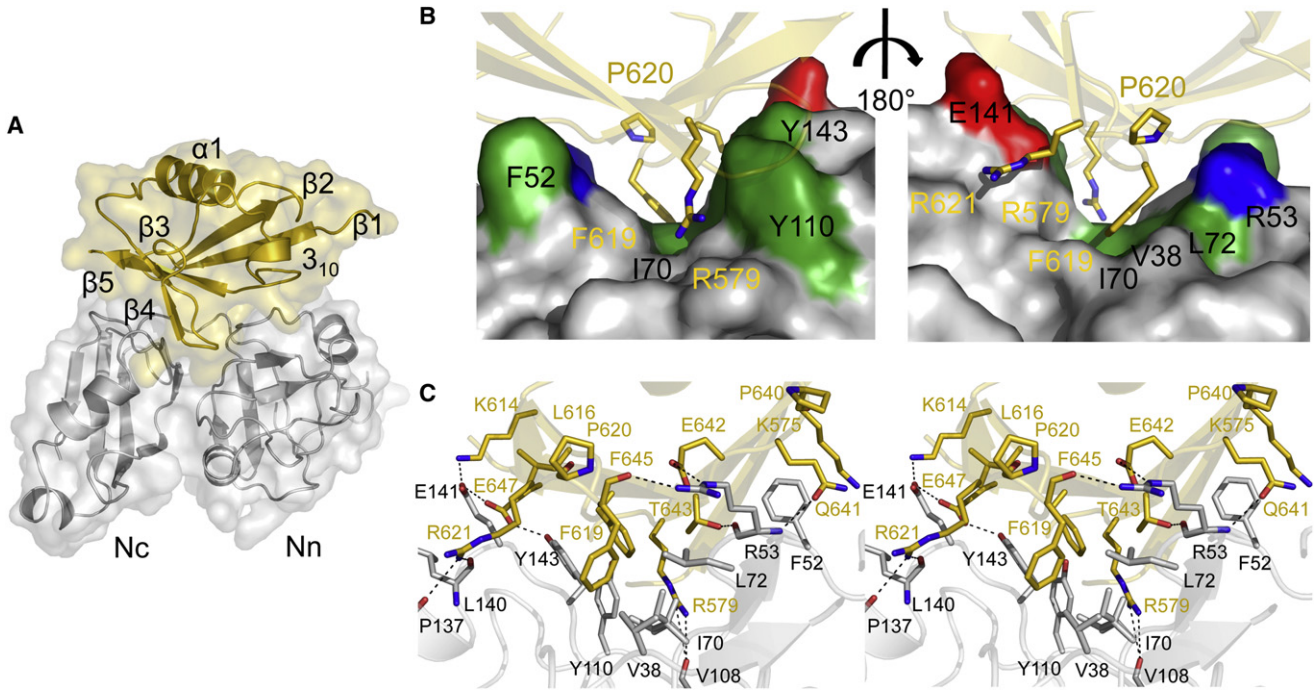

Figure 1. Structure of p97N in Complex with the UBX Domain of FAF1

(A) Ribbon and surface representation of the overall structure. The UBX domain is shown in gold and p97N in gray.

(B) Surface representation of the binding pocket on the N domain. The UBX domain and p97N are colored as in (A). Hydrophobic residues of p97 are colored in green, acidic residues in red, and basic residues in blue.

(C) Stereo view of the interface. Residues involved in binding are shown in stick representation. Carbon atoms of p97 residues are colored in gray and for FAF1UBX in gold. Dashed lines indicate H bonds.

the long distance by the program PDBePISA (Figure 1C). In addition to its S3/S4 loop, UBX binds via its N-terminal β strand S1 (Lys575, Arg579) and its C-terminal β strand S5 (Gln641, Glu642, Thr643, Phe645, Glu647) to p97 (Figure 1C). Residues from connecting loops of both subdomains of p97 contribute to the p97-FAF1 interface. These residues contact the surface of the UBX β sheet in the region around β strands 1, 3, 4, and 5.

This binding mode of p97 in which it interacts with the hydrophobic surface of the UBX β sheet resembles the recognition of ubiquitin by a large number of so-called ubiquitin-binding domains (UBDs) (Dikic et al., 2009). UBDs are structurally diverse motifs that recognize and bind to ubiquitin as well as proteins sharing the ubiquitin-like fold such as the UBX domain. Most UBDs use α-helical structures to bind to the hydrophobic patch in the β sheet of ubiquitin centered on Ile44. Ile44 corresponds to Leu616 in FAF1UBX, and this residue is located in β strand S3 that precedes the S3/S4 loop. In contrast to the α-helical UBDs, the p97 interaction site is located in the cleft between the two N-terminal subdomains, and p97 recognizes the corresponding hydrophobic patch via loop elements. Therefore, this interaction is distinct from that observed for canonical UBDs.

The Conserved R…FPR Signature of FAF1UBX Features a *cis*-Proline

The structures of the N domain of p97 in its apo state and in complex with the FAF1UBX domain can be superimposed with a root-mean-square deviation (rmsd) of 0.7 Å. Nevertheless, subtle conformational changes induced by UBX binding are obvious. Phe52, Arg53, and Glu141 show significant differences in the orientations of their side chains (see Figure S1 available online). All three side chains in the apo structure are flipped away from the putative interaction interface, whereas they are involved in either hydrogen bonding or hydrophobic interactions in the p97N-FAF1UBX structure.

A closer examination of the p97N-FAF1UBX complex structure revealed that two proline residues, Pro620 in the conserved and essential S3/S4 loop as well as the nonconserved Pro640 in the 3_{10}/S5 loop, adopt the *cis*-isomer in the complex structure. To investigate whether theses proline residues are already in the *cis*-configuration prior to p97 binding, or whether this interaction induced a *trans*- to *cis*-isomerization, we also determined the apo structure of FAF1UBX. This structure was solved by molecular replacement with the FAF1UBX domain of the p97N-FAF1UBX complex crystal structure as search model, and was refined at 3.0 Å resolution to a crystallographic R factor of 17.8% and a free R factor of 25.8% (Table 1). Four FAF1UBX monomers (referred to as A–D) are present in the asymmetric unit. The four FAF1UBX molecules can be superimposed onto the corresponding residues in the p97N-FAF1UBX complex with an rmsd of 0.60 Å (A), 0.85 Å (B), 0.64 Å (C), and 0.74 Å (D) calculated over 80 aligned residues. Interestingly, in all four monomers Pro640 is already in the *cis*-configuration (Figures 2A and 2B). However, the superimposed structures revealed differences for the FPR loop containing Pro620. This region

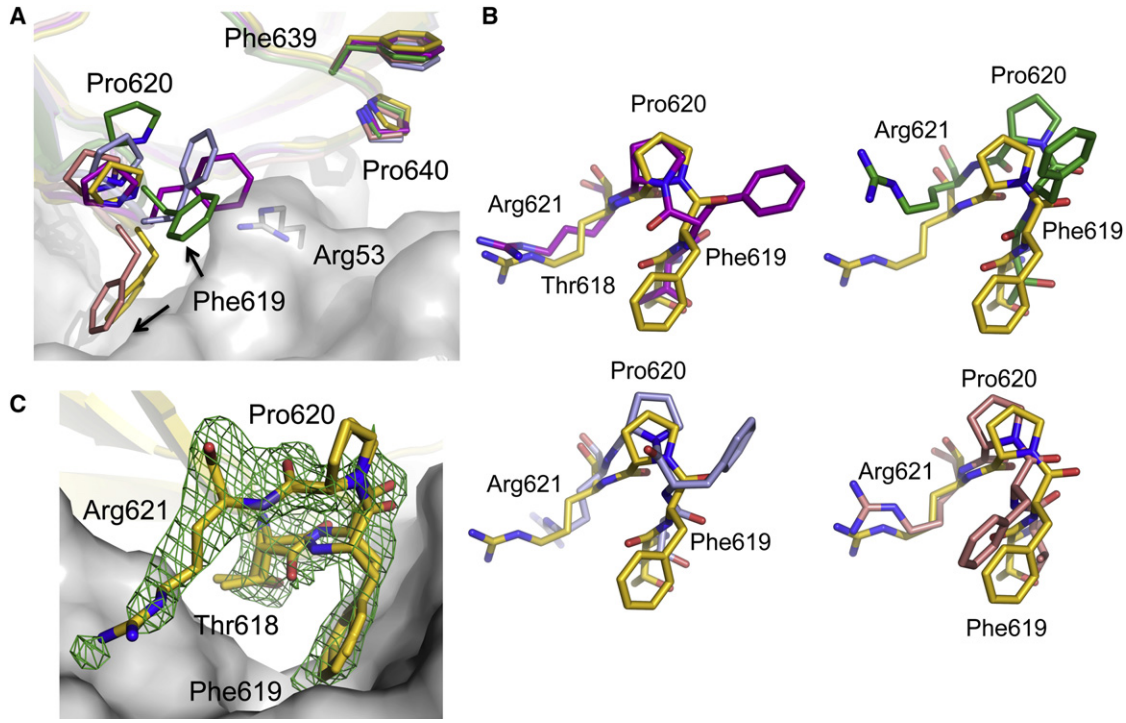

Figure 2. Comparison of FAF1UBX in Complex with p97N and in the Apo State

(A) Superposition of the FAF1UBX apo structure with FAF1UBX in complex with p97N (colored in gold) shown as a ribbon representation (see also Figure S1). The four UBX monomers present in the asymmetric unit are superimposed and are colored in purple (chain A), green (chain B), blue (chain C), and pink (chain D). p97N is shown in a surface representation. The two Phe-Pro dipeptides containing the *cis*/*trans* bonds are shown in stick representation.

(B) The *trans*- and *cis*-isomers of Pro620 in the apo structure are superimposed onto the corresponding residues in the complex structure and are colored as in (A).

(C) SIGMAA-weighted F_o-F_c omit electron density map of the S3/S4 loop contoured at three times the rmsd. Residues 618–621 were omitted from the model.

displays significant conformational variability with two of the molecules (chains B and D) having the critical FPR loop in the *cis*-configuration and the remaining two (A and C) in the *trans*-configuration. In the B chain the loop is stabilized by an adjacent molecule, whereas it is more solvent exposed in chain D as it is in chains A and C. This indicates that the FAF1UBX domain in the absence of p97 displays conformational variability with Pro620 being present in both the *cis*- and *trans*-configuration and that p97 selects the *cis*-isomer upon binding. The *cis*-configuration of Pro620 seems to be essential for binding of the FAF1UBX domain to p97 because the *trans*-isomer would lead to either severe steric clashes with Arg53 of p97N, or Phe619 would not stretch into the binding cleft and would stay solvent exposed (Figure 2A). Because Phe619 is one of the key residues in p97 interaction, this would disrupt the binding of the FAF1UBX domain to p97 (see below). The observations regarding the mixture of *cis*- and *trans*-isomers in the isolated state are in excellent agreement with another crystal structure of the FAF1UBX domain, which has just been published (Kang and Yang, 2011).

In contrast to the FAF1UBX structure, in the UBX domain of p47 in complex with p97ND1 (Dreveny et al., 2004), the crucial proline in the S3/S4 loop has been modeled in the *trans*-configuration. In this structure the conserved FPR loop can theoretically bind into the hydrophobic N domain pocket with the proline in either *cis* or *trans*, which is due to the fact that in the UBX domain of p47, the second arginine of the conserved R…FPR motif is replaced by asparagine. The shorter side chain of this residue would allow for enough rotational/conformational flexibility to adopt both configurations in the complex. In contrast the longer side chain of FAF1 Arg621 that compacts the loop most likely requires the *cis*-isomer. In our p97N-FAF1UBX crystal structure, a partial disorder of this loop resulting in a conformational heterogeneity is observed despite the unambiguous assignment of the *cis*-proline. Although this loop was modeled in two conformations that differ by a flip in the peptide between residues Thr618 and Phe619 (Figure 2C), weak additional difference density is still visible, reflecting an increased mobility that might be important for interaction. Interestingly, the solution structure of the UBX domain of UBXD7 (PDB entry 2DLX), which shares 35% sequence identity with FAF1UBX, features both prolines (Pro620 and Pro640 of FAF1) in the *cis*-configuration.

A Conserved Binding Mode for p97N Adaptor Proteins

The structures of p97N in complex with the FAF1UBX domain (this study) as well as the structure of p47UBX-p97ND1 (Dreveny et al., 2004) and an NMR-derived model of the NPL4 N-terminal ubiquitin-like domain (ULD) in complex with p97N (Isaacson et al., 2007) show that, so far, all characterized adaptor proteins bind to the same hydrophobic cleft formed between the two N-terminal subdomains of p97 (Figure 3A). As mentioned earlier,

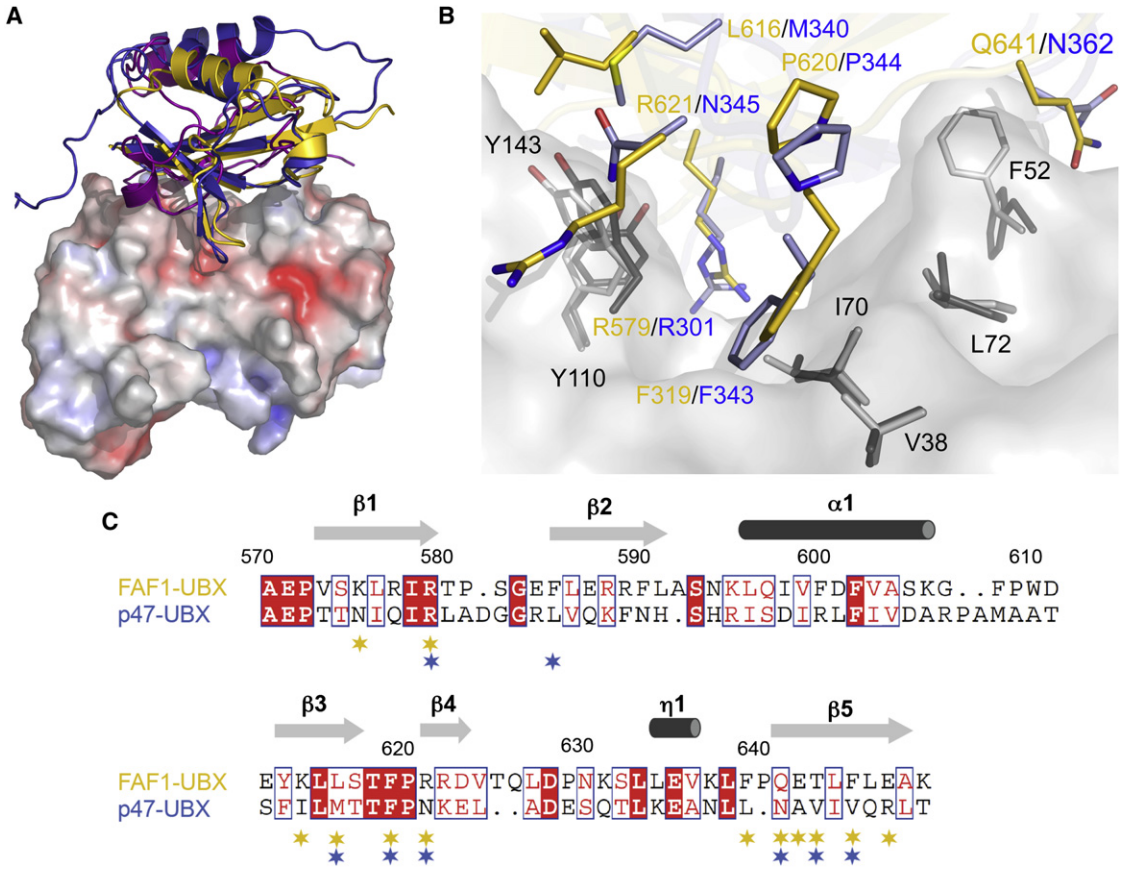

Figure 3. Adaptor Protein Binding to p97

(A) Ribbon representations together with the molecular surface of p97N colored according to electrostatic potential (electropositive in blue, electronegative in red, contoured at ± 10 kT) in complex with FAF1UBX (this study, gold), p47UBX (PDB entry 1S3S, colored in blue), and NPL4 ULD (PDB entry 2PJH, colored in magenta).

(B) Close-up view showing the common p97N-binding surface important for FAF1UBX and p47UBX interaction. Key residues involved in the respective interaction are shown in a stick representation with p97N in light (FAF1UBX complex) and dark gray (p47UBX complex), FAF1UBX in gold, and p47UBX in blue.

(C) Structure-based sequence alignment of the FAF1UBX and p47UBX domains. Secondary structure elements of FAF1UBX were assigned using DSSP (Kabsch and Sander, 1983) and are labeled above the sequences. The alignment was performed using DaliLite (Holm et al., 2008), and the figure was prepared with ESPript (Gouet et al., 1999). Strictly conserved amino acids are highlighted with a red background and similar amino acids as red letters. Residues involved in p97 interaction are labeled with gold stars (FAF1UBX) and blue stars (p47UBX).

UBX domain-containing proteins constitute the largest family of p97 adaptor proteins (Schuberth and Buchberger, 2008), and the structures of the UBX domains of FAF1 and p47 are likely to represent a general p97-binding mechanism for all UBX proteins. The crystal structures of the FAF1 and p47 UBX domains in complex with p97 can be superimposed with an rmsd of 1.8 Å, and both UBX domains bind via the conserved UBX R…FPR (R…FPN in p47) motif (Figures 3B and 3C). Additional interacting residues located in β strands S1 and S5 are not as strongly conserved (Figure 3C). Both proteins bind in a similar manner to the p97 interdomain cleft, mediated mainly via hydrophobic interactions with residues Val38, Phe52, Ile70, Leu72, Tyr110, and Tyr143 of p97N.

The NPL4 ULD resembles ubiquitin rather than UBX in the length of its S3/S4 loop but contains an additional 3_{10}-helical insert that provides specific contacts with p97, which distinguishes it from both ubiquitin and the UBX domain. The β sheet of the NPL4 ULD is oriented in such a way that it covers the hydrophobic-binding groove (Figure 3A). Nevertheless, all these ULDs recognize the p97N cleft using similar, yet subtly different interaction modes. p97N residues common to all interactions are Phe52, Tyr110, and Tyr143. The loop in ubiquitin that corresponds to the UBX S3/S4 loop is shorter by two residues, which correspond precisely to the Phe619-Pro620 dipeptide. In addition, Arg621 is replaced by a glycine that results in a sharp turn. This might explain why monoubiquitin binds to p97 with only low affinity (Rape et al., 2001), although it shares the same overall fold.

FAF1 Assembles into a Ternary Complex with p97 and UFD1/NPL4 via Its UBX Domain

Both the UBA-UBX protein p47 and the heterodimeric UFD1/NPL4 cofactor use a similar bipartite mechanism that involves binding via the UBX domain (p47) or ULD (NPL4) and a Shp box (p47 or UFD1) to the N domain of p97, and hence, both cofactors compete for p97 binding in vitro (Bruderer et al.,

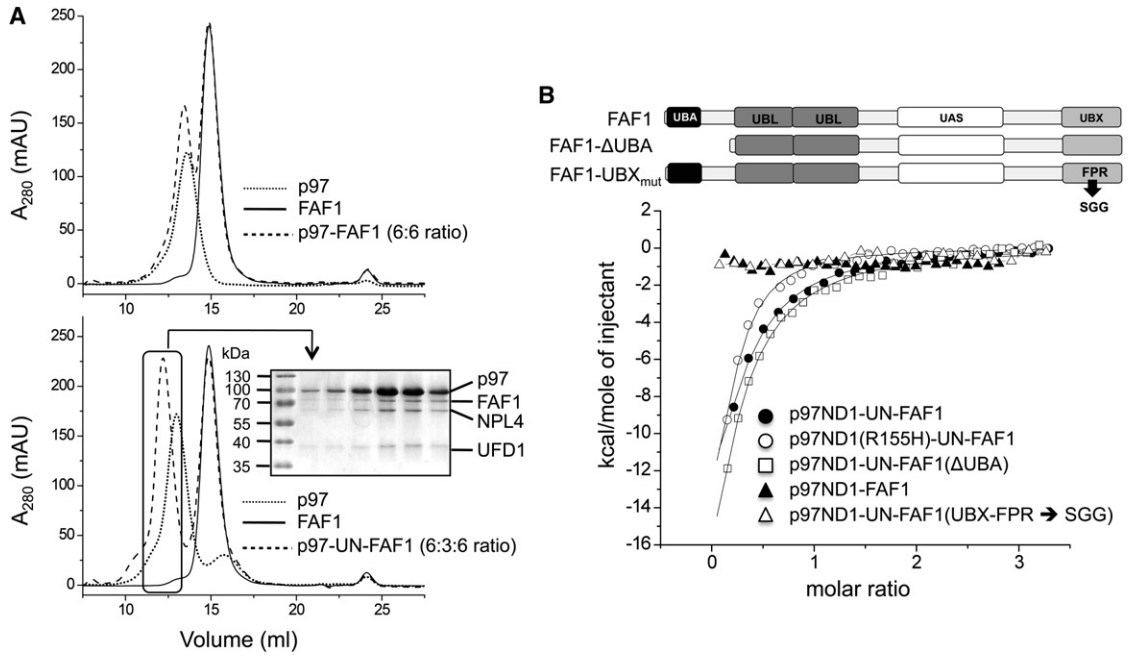

Figure 4. Interaction of p97 with FAF1

(A) Analytical size exclusion chromatography of p97-FAF1 (upper panel), p97-UFD1/NPL4-FAF1 (bottom panel), and the individual components. p97 (5 μM) was incubated with UFD1/NPL4 and FAF1 in a 6:3:6 molar ratio. The indicated elution fractions were analyzed by SDS-PAGE followed by Coomassie brilliant blue staining.

(B) ITC analysis of p97ND1-FAF1 and variants. The domain architecture of FAF1 is shown on top, and the FAF1 variants are indicated. UN, UFD1/NPL4.

2004; Meyer et al., 2000). p47 binds as a trimer where each monomer is associated with two adjacent p97 protomers (Beuron et al., 2006). In contrast only one UFD1/NPL4 heterodimer binds to two adjacent protomers of a p97 hexamer (Pye et al., 2007), thus potentially allowing further cofactors to bind to nonoccupied N domains. Accordingly, it could be shown that other UBA-UBX proteins like Ubx2, FAF1, and UBXD7 coimmunoprecipitate p97 with the UFD1/NPL4 heterodimer and endogenous ubiquitin conjugates (Alexandru et al., 2008; Schuberth and Buchberger, 2005), an observation that is consistent with the existence of higher-order complexes. We consequently characterized the putative ternary p97-UFD1/NPL4-FAF1 complex in more detail. Initially, we analyzed the in vitro interaction between FAF1 and p97 by analytical size exclusion chromatography (Figure 4A). Under these conditions complex formation surprisingly was only observed in the presence of UFD1/NPL4. Analysis of this ternary complex by SDS-PAGE suggests a substoichiometric binding of FAF1 and UFD1/NPL4 with respect to the number of p97 protomers.

To determine the affinity of the interaction between p97-UFD1/NPL4 and FAF1 as well as the exact stoichiometry of this complex, we used isothermal titration calorimetry (ITC) (Figure 4B and Table 2). Because ITC analyses with both full-length p97 as well as p97ND1, which lacks the second ATPase domain, revealed no differences in binding affinity, further experiments were conducted with the truncated hexameric p97ND1 protein. Again, under these conditions no binding of FAF1 to p97 could be detected in the absence of UFD1/NPL4. Analysis of the exothermic-binding curve in the presence of UFD1/NPL4 showed that the best fit is obtained with a one-site binding model, yielding a binding stoichiometry (N) for the p97/p97ND1 hexamer of N = 0.18 ± 0.05/0.11 ± 0.07, which is consistent with the binding of one FAF1 molecule to the p97/p97ND1 hexamer and a dissociation constant (K_D) of 2.3 ± 0.22/2.6 ± 0.35 μM. Under the same conditions we could confirm a 6:3 binding stoichiometry (N = 0.38 ± 0.01/0.34 ± 0.01) and a K_D of 0.70 ± 0.04/0.54 ± 0.02 μM for the interaction between trimeric p47 and p97/p97ND1, in agreement with published data (Beuron et al., 2006). Analysis of the binary p97/p97ND1-UFD1/NPL4 interaction confirmed the proposed 6:1 stoichiometry (N = 0.15 ± 0.02/0.11 ± 0.03) and a K_D of 1.7 ± 0.20/2.1 ± 0.18 μM.

Earlier immunoprecipitation experiments showed that the FAF1 UBX domain is crucial for the interaction with endogenous p97 (Song et al., 2005). However, at this point it has not been analyzed whether the multidomain protein FAF1, like p47, uses a bipartite-binding mechanism involving two separate FAF1-binding sites or whether its UBX domain solely mediates the interaction with p97-UFD1/NPL4. A FAF1 variant lacking the N-terminal substrate-binding UBA domain has no effect on complex formation (Figure 4B and Table 2). Furthermore, a FAF1UBX variant, in which the conserved FPR motif was replaced by the SGG motif found in UBXD1 (Carim-Todd et al., 2001), a UBX protein that does not interact with p97 via its UBX domain (Kern et al., 2009; Madsen et al., 2008), completely abolished binding under these conditions (Figure 4B and Table 2). This result clearly demonstrates that the interaction of FAF1 with p97-UFD1/NPL4 is not mediated by a bipartite-binding mechanism and that the UBX domain constitutes the only binding determinant.

It has been proposed that ATP binding/hydrolysis triggers conformational changes of the p97N domain that are important

Table 2. ITC Parameters of p97, p97-UFD1/NPL4, and Interaction Partners

		K_D (μM)	N	ΔG (kcal/mol)
p97ND1	flFAF1	n.d.	n.d.	n.d.
flp97-UN	flFAF1	2.3 ± 0.22	0.18 ± 0.05	−7.9
p97ND1-UN	flFAF1	2.6 ± 0.35	0.11 ± 0.07	−8.0
flp97	p47	0.70 ± 0.04	0.38 ± 0.01	−8.5
p97ND1	p47	0.54 ± 0.02	0.34 ± 0.01	−8.6
flp97	UFD1/NPL4	1.7 ± 0.20	0.15 ± 0.02	−8.1
p97ND1	UFD1/NPL4	2.1 ± 0.18	0.11 ± 0.03	−8.0
p97ND1-UN	ΔUBAFAF1	2.2 ± 0.33	0.11 ± 0.08	−7.9
p97ND1(R155H-Mg^{2+}/ATPγS)-UN[a]	flFAF1	1.14 ± 0.07	0.17[b]	−8.2
p97ND1-UN	flFAF1UBX(FPR → SGG)	n.d.	n.d.	n.d.
flp97-UN	flUBXD7	3.1 ± 0.40	0.22 ± 0.08	−7.6
p97ND1-UN	flUBXD7	2.0 ± 0.24	0.24 ± 0.06	−7.9
p97ND1-UN	FAF1UBX	1.5 ± 0.42	0.27 ± 0.06	−7.9

All numbers shown are averages of two experiments using independent protein preparations. The errors represent the larger experimental uncertainty of the two measurements given by the Origin software following curve fitting of the experimental data. N, binding stoichiometry; n.d., no binding detected; UN, UFD1/NPL4; fl, full-length.

[a] Single experiment with experimental errors.

[b] N value was fixed before fitting the data to allow accurate determination of the other parameters.

for adaptor protein binding/release (Rouiller et al., 2000). Analysis of adaptor protein binding to p97 in the presence or absence of ATP is complicated due to the fact that isolated p97 typically has ADP bound at its D1 domain, which cannot be exchanged (Pye et al., 2006). Recently, it has been shown that IBMPFD variants undergo a nucleotide-induced conformational change of the N domain (up and down conformation) in the presence of the nonhydrolyzable ATP analog ATPγS (Tang et al., 2010). However, analysis of the p97-R155H variant, the most common missense mutation found in patients with IBMPFD, did not alter significantly (2-fold affinity increase) the binding behavior of UDF1/NPL4 and FAF1 to p97 in the presence of ATPγS (Figure 4B and Table 2), thus indicating that a general conformational change of the N domain is not crucial for triggering association/dissociation of these adaptor proteins but could be important for interaction with substrates or other proteins.

An analysis of the p97/p97ND1 interaction with UBXD7, another UBA-UBX protein, revealed the same UFD1/NPL4-dependent binding behavior resulting in a 6:1:1 stoichiometry for the ternary p97-UFD1/NPL4-UBXD7 complex with a binding stoichiometry of N = 0.22 ± 0.08/0.24 ± 0.06 and a K_D of 3.1 ± 0.40/2.0 ± 0.24 μM (Table 2). Based on analytical size exclusion chromatography, ITC, and crosslinking experiments (data not shown), a stable UFD1/NPL4-FAF1 interaction has not been observed, suggesting that p97 undergoes conformational changes upon binding of UFD1/NPL4 that allow for the subsequent binding of FAF1. The data presented here reveal a hierarchy in cofactor binding with the UFD1/NPL4 heterodimer preceding the UBA-UBX proteins.

Analysis of the p97N-FAF1UBX Complex Interface

To further probe the interaction between FAF1 and p97, we analyzed the importance of interface residues identified in the p97N-FAF1UBX complex structure by site-directed mutagenesis and subsequent binding assays using p97ND1 and FAF1UBX variants. The contribution of these residues was initially studied in pull-down binding assays in the absence of UFD1/NPL4. In contrast to full-length-FAF1, binding of the isolated UBX domain does not strictly depend on the presence of this cofactor, which also explains why we were able to obtain the complex structure. However, one should keep in mind that protein concentrations during crystallization were significantly higher than during ITC and size exclusion chromatography experiments, thus compensating for the reduced affinity of the p97-FAF1 interaction in the absence of UFD1/NPL4. Residues involved in hydrophobic interactions (Val38, Phe52, Ile70, Leu72, and Tyr110) revealed a significantly reduced binding to FAF1UBX (Figure 5A). Interestingly, the exchange of Arg53, which apparently stabilizes the conformation of the S3/S4 loop, with alanine does not lead to a destabilization of the complex, indicating that hydrophobic interactions, although they only constitute 25% of the binding interface, are the key driving forces for this interaction. Analysis of FAF1UBX variants showed a largely reduced binding for residues located in the conserved ^{579}R…^{619}FPR^{621} motif (Figure 5B).

ITC studies with p97ND1 and the UBX domain of FAF1 revealed only a weak exothermic reaction and low binding affinity resulting in a K_D value of 30 μM. Similar to full-length FAF1, the isolated UBX domain also needs UFD1/NPL4 for high-affinity binding (K_D = 1.5 ± 0.42 μM) (Table 2). To allow for a direct comparison with the wild-type complex, the UFD1/NPL4 heterodimer in complex with p97ND1 was utilized for analysis of the UBX variants. The ITC experiments confirmed the results obtained in the pull-down assays with variants of the ^{579}R…^{619}FPR^{621} motif exhibiting affinities, which are reduced by a factor of 8–13 (Figure 5C). The K_D values are 18 μM for R579A, 20 μM for F619A, and 12 μM for R621A compared to wild-type UBX with a K_D of 1.5 μM, whereas the F645A variant with a K_D of 1.6 μM showed no effect (Figure 5C). As shown above, the conserved Pro620 in the S3/S4 loop, as well as

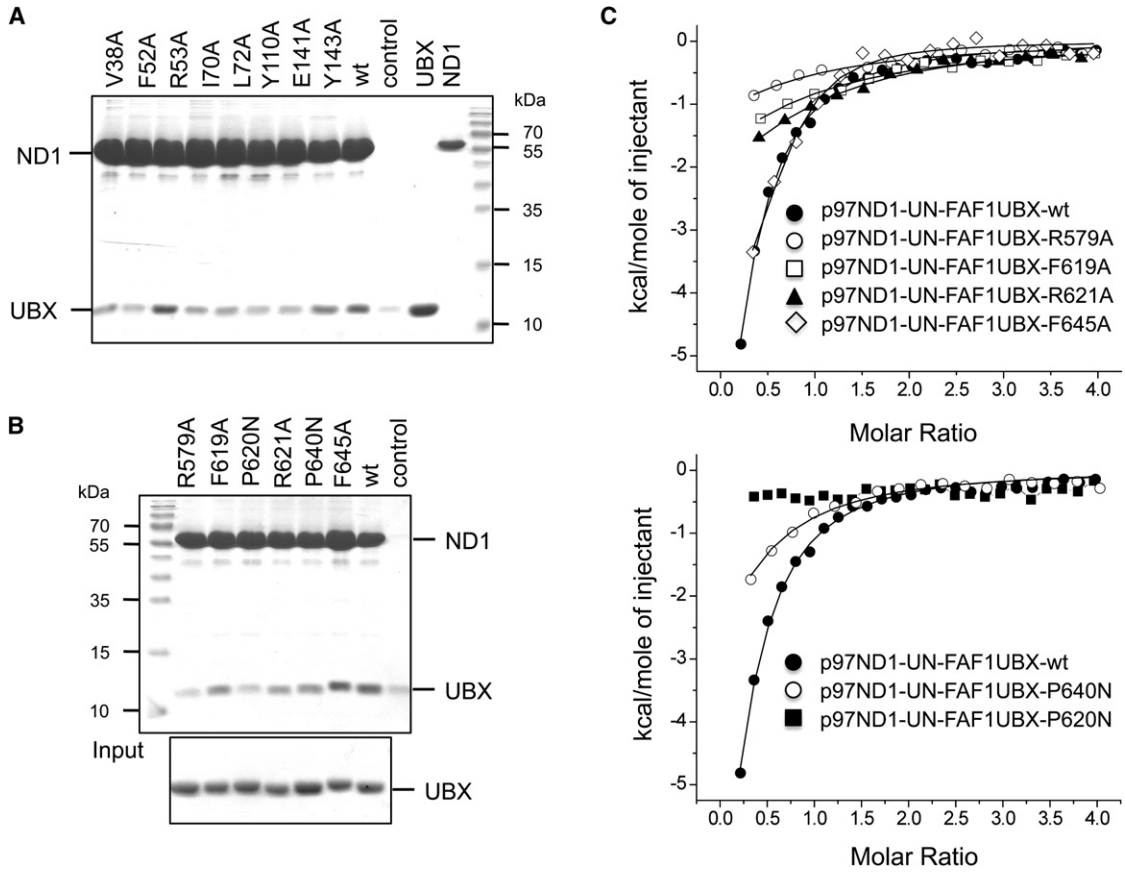

Figure 5. Analysis of the p97N-FAF1UBX Interface

(A) His-tag pull-down assays of p97ND1 variants: His-tagged p97ND1 wild-type (WT) and indicated variants were used. Binding of FAF1UBX WT was analyzed by SDS-PAGE of the reaction mixture followed by Coomassie brilliant blue staining. FAF1UBX alone was included as a control to estimate the amount of nonspecific UBX binding (labeled control), and a loading control for FAF1UBX (labeled UBX) is shown.

(B) His-tag pull-down assays of FAF1UBX variants: His-tagged p97ND1 WT was used. Binding of FAF1UBX WT and indicated variants was analyzed as in (A).

(C) ITC analysis of FAF1UBX binding to p97ND1 in the presence of UFD1/NPL4 (UN) and UBX mutants.

Pro640 in the 3_{10}/S5 loop, is in the *cis*-configuration, which seems to be important for interaction with p97 (Figure 2). Indeed, an exchange of either FAF1UBX proline (Pro620 or Pro640) with asparagine, a residue that strongly favors the *trans*-conformation yet can stabilize β turns via backbone hydrogen bonds, completely abolished binding under these conditions in the case of Pro620 as measured by ITC, or caused a 7-fold reduction in affinity in the case of Pro640 with a K_D of 10 μM for the P640N mutant compared to 1.5 μM for the wild-type (Figure 5C). Due to the fact that NPL4 and the UBX domain of FAF1 share overlapping binding sites (see above), the p97ND1 variants could not be analyzed by ITC because they would also prevent binding of UFD1/NPL4.

DISCUSSION

UBX domain-containing cofactors represent the largest group of p97-binding partners. At present only the structure of the p97ND1-p47UBX complex is available; however, the UBX domain of p47 deviates from the canonical R…FPR motif in the last residue, which is asparagine instead of arginine. In agreement with the p97-p47 complex, our data show that the crucial determinants of UBX domain binding to the N domain of p97 are provided by the UBX ^{579}R..^{619}FPR^{621} signature motif (residue numbers refer to the FAF1 UBX domain). In contrast to the UBX domain of p47, the FPR motif adopts a *cis*-proline configuration, which, based on site-directed mutagenesis data, is essential for binding and allows the aromatic ring of Phe619 to insert into the hydrophobic interdomain cleft of p97N. Both arginines deeply stretch into the p97-binding pocket to anchor the UBX domain and to stabilize the complex by essential hydrophobic interactions (Figure 1C). Nearly all UBX domains contain an arginine, or less frequently a lysine, at the position corresponding to Arg579 of FAF1, and a hydrophobic residue followed by a proline in the S3/S4 loop, thus indicating the functional importance of these residues (Buchberger et al., 2001). The second arginine (Arg621 in FAF1) is conserved in all UBA-UBX proteins with the exception of p47, and we predict that in those proteins the proline is always in the *cis*-configuration.

One of the key questions regarding the biological function of p97 is how this highly versatile ATPase participates in many dissimilar physiological processes. It is clear that answers to this question can only be gained by studying the interaction of p97 and its structurally diverse adaptor proteins. It has been

reported that some adaptor proteins that target identical or overlapping sites on p97 bind in a mutually exclusive manner, including the substrate-recruiting cofactors p47 and UFD1/NPL4 (Bruderer et al., 2004; Meyer et al., 2000). However, these proteins can combine with additional cofactors to form distinct assemblies of p97-protein complexes (Alexandru et al., 2008; Schuberth and Buchberger, 2008), as shown in this study for the p97-UFD1/NPL4-FAF1 and p97-UFD1/NPL4-UBXD7 complexes, thus suggesting that simple competition for p97-binding sites is unlikely to be the only determinant in cofactor selectivity. Although it has been proposed that nucleotide-induced conformational changes of the p97N domain can trigger assembly/disassembly of adaptor proteins (Rouiller et al., 2000), our studies with the most prevalent IBMPFD variant (p97-R155H) suggested that a general conformational change of the N domain is not crucial for association/dissociation of the FAF1 or UBXD7 adaptor proteins.

Instead, our data clearly demonstrate a hierarchical binding to p97 for the two UBA-UBX containing adaptor proteins. Two distinct mechanisms could explain why binding of the UBX domain-containing cofactors FAF1 and UBXD7 require preassembly of the UFD1/NPL4 heterodimer with p97: (1) the UFD1/NPL4 complex when bound to p97 provides additional interaction sites for FAF1 and UBXD7 so that high-affinity binding of these proteins requires not only the complementary surface between p97 and the UBX domain described in this work but also a direct interaction between UFD1/NPL4 and the UBA-UBX containing cofactors FAF1 and UBXD7; and (2) binding of UFD1/NPL4 induces conformational changes in p97, resulting in an asymmetry in p97 so that only one of the vacant p97 subunits interacts tightly with FAF1 or UBXD7. According to this model, FAF1/UBXD7 binding does not have to occur adjacent to the UFD1/NPL4 heterodimer but requires the presence of the UFD1/NPL4 cofactor. Our data currently do not allow us to formally rule out one of these models. However, the observation that binding of the isolated UBX domain of FAF1 to p97 also requires the presence of UFD1/NPL4 renders the first model less likely because a potential UFD1/NPL4-FAF1 interaction would be restricted to the UBX domain, which constitutes only one-eighth of the total FAF1 residues. This assumption is also supported by our inability to crosslink the UFD1/NPL4-FAF1 proteins. Nevertheless, additional biochemical and structural studies are required to establish the molecular details of the hierarchy in cofactor binding to p97 described here for the first time.

The hierarchical binding of cofactors to p97 provides an additional layer of specificity control for cellular processes involving UFD1/NPL4. As was first shown for yeast Ubx2, UBA-UBX cofactors have the potential to regulate the subcellular localization and/or substrate range of the p97-UFD1/NPL4 complex (Neuber et al., 2005; Schuberth and Buchberger, 2005, 2008). Such a control mechanism is not only consistent with the hierarchical binding model described here but in fact critically requires it. Otherwise, yeast Ubx2 and other UBA-UBX cofactors would be able to recruit p97 complexes lacking UFD1/NPL4, which, at least in the case of Ubx2 and the ERAD pathway, would result in nonfunctional, potentially dominant-negative p97 assemblies. Conversely, the hierarchical binding model predicts that cellular functions of yeast Ubx2, mammalian FAF1, and UBXD7 should strictly depend on UFD1/NPL4. While this is clearly the case for Ubx2, an involvement of UFD1/NPL4 in the UBXD7-dependent turnover of HIF-1α and in the degradation of FAF1 targets remains to be addressed experimentally. Interestingly, a number of additional mammalian UBA-UBX proteins were found to bind to p97 and UFD1/NPL4 (Alexandru et al., 2008), suggesting that they also could bind in a hierarchical manner to the p97-UFD1/NPL4 complex to direct it to still unknown targets.

EXPERIMENTAL PROCEDURES

Cloning and Site-Directed Mutagenesis

The following constructs were used in this study: full-length FAF1 (aa 1–650), FAF1ΔUBA (aa 98–650), and FAF1UBX (aa 568–650) (pETM11, EMBL Heidelberg, PciI/XhoI, N-terminal His-tag); full-length p97 (aa 1–806) and p97N (aa 1–187) (pProEx_HTA, Invitrogen, KasI/HindIII, N-terminal His-tag); p97ND1 (aa 1–480) (pET21b, Novagen, NdeI/SalI, C-terminal His-tag); UBXD7 (modified pRSET A, Invitrogen, BamHI/EcoRI, N-terminal His-tag); UFD1 (pET-Duet, Novagen, NcoI/HindIII, N-terminal His-tag); and NPL4 (pCOLA-Duet, Novagen, NcoI/EcoRI). For site-directed mutagenesis of FAF1UBX and p97ND1, the QuikChange® II Site-Directed Mutagenesis Kit from Agilent was used.

Protein Expression and Purification

All proteins were expressed in *E. coli* BL21(DE3) RIL cells (Novagen) by induction with 0.5–1 mM IPTG at an OD_{600} of 0.6 overnight at 16°C. UFD1 and NPL4 were coexpressed. Proteins were purified in 50 mM Tris (pH 8), 150 mM KCl, 5% (v/v) glycerol, 5 mM $MgCl_2$ buffer (buffer A), and 5 mM β-mercaptoethanol by metal affinity chromatography (Ni-NTA, Invitrogen; Ni-TED, Macherey-Nagel) and size exclusion chromatography (Superdex 200, Superose 6, GE Healthcare). Prior to size exclusion chromatography, FAF1UBX, full-length p97, and its N domain were dialyzed at 4°C overnight in the presence of TEV protease (1:50) followed by Ni-NTA chromatography to remove uncleaved proteins as well as His-tagged TEV protease. All proteins were concentrated to ~10 mg/ml by ultrafiltration (Vivaspin, Sartorius), shock frozen, and stored at −80°C.

Crystallization

For crystallization of the p97N domain in complex with the FAF1UBX domain, both proteins were incubated at a molar ratio of 1:2 for 1 hr at 4°C and concentrated to 10 mg/ml. Crystals were grown by vapor diffusion in hanging drops containing equal volumes of protein in buffer A and 5 mM dithiothreitol (DTT), and a reservoir solution consisting of 16%–20% (w/v) polyethylene glycol monomethyl ether 2000, 0.2 M trimethyl-N-oxide and 0.1 M Tris (pH 8.5) equilibrated against the reservoir solution. Crystals belong to space group $P6_5$ with approximate cell dimensions of a = b = 88.1 Å and c = 66.9 Å with one complex per asymmetric unit. Crystals of the p97N domain (9.5 mg/ml) were obtained in 1 M 1,6-hexanediol, 0.1 M Na-acetate (pH 4.5), and 0.01 M $CoCl_2$. They belong to space group $P3_1$ with approximate cell dimensions of a = b = 60.6 Å and c = 63.1 Å with one molecule per asymmetric unit. Crystals of the FAF1UBX domain (50 mg/ml) were obtained in 0.4 M NaH_2PO_4/1.6 M K_2HPO_4, 0.1 M imidazole (pH 8.0) and 0.2 M NaCl, which belong to space group $P6_1$ with approximate cell dimensions of a = b = 92.6 Å and c = 108.5 Å containing four molecules per asymmetric unit.

Data Collection and Structure Determination

Crystals were cryoprotected by soaking in mother liquor supplemented with 15%–30% (v/v) glycerol, flash cooled in liquid nitrogen, and data collection was performed at 100 K. Data were collected at beamlines BL 14.1 (BESSY, Berlin) and ID23-1 (ESRF, Grenoble) and processed using iMosflm and Scala (Evans, 2006; Leslie, 1992). Data collection statistics are summarized in Table 1. For subsequent calculations the CCP4 suite and PHENIX were utilized (Adams et al., 2010; CCP4, 1994) with exceptions as indicated. The structures were solved by molecular replacement using *Phaser* (McCoy et al., 2007) with the N domain of p97 (PDB entry 1S3S) and the UBX domain of FAF1 (PDB entry 1H8C) as search models. The structure of apo FAF1UBX was solved with the FAF1UBX crystal structure (this work) as search model. The structures were refined with PHENIX incorporating TLS refinement. Solvent molecules were automatically added with PHENIX. For model building

and fitting, Coot was used (Emsley and Cowtan, 2004). The figures were generated with PyMOL (http://www.pymol.org).

In Vitro Binding Assays

For pull-down assays, His-tagged p97ND1 and variants were immobilized on Ni-NTA beads. In all experiments, 40 μl of beads were incubated with 5 μM of purified p97ND1 in 400 μl of Tris-buffered saline (TBS) with 1 mM DTT and 0.1% (v/v) Triton X-100 at 4°C for 2 hr. After centrifugation (1250 × g, 30 s), beads were washed four times with 400 μl of binding buffer. Purified UBX proteins (25 μM) in a total volume of 400 μl of binding buffer were added to immobilized p97ND1 and treated in the same way as in the first step. Immobilized proteins were directly analyzed by 18% (v/v) SDS-PAGE. FAF1UBX alone was included as control to estimate the amount of nonspecific UBX binding. ITC experiments were conducted as described (Hänzelmann et al., 2010) using 50 mM Tris (pH 8), 150 mM KCl, and 1 mM β-mercaptoethanol as buffer. In all experiments, 75–150 μM of ligands was titrated into the sample cell containing 5–10 μM of full-length p97/p97ND1 or full-length p97/p97ND1-UFD1/NPL4. Complex formation was analyzed by analytical size exclusion chromatography (Superose 6, GE Healthcare). p97 (5 μM) or p97-UFD1/NPL4 (6:3 molar ratio) was incubated with FAF1 at a 6:6 (p97:FAF1) molar ratio for 1 hr on ice. Size exclusion chromatography experiments were performed in 50 mM Tris (pH 8.0), 150 mM KCl, and 1 mM β-mercaptoethanol.

ACCESSION NUMBERS

Atomic coordinates and structure factors have been deposited in the Protein Data Bank at RCSB with accession codes 3QQ7, 3QQ8, and 3R3M.

SUPPLEMENTAL INFORMATION

Supplemental Information includes one figure and can be found with this article online at doi:10.1016/j.str.2011.03.018.

ACKNOWLEDGMENTS

This work was supported by the Deutsche Forschungsgemeinschaft (Rudolf Virchow Center for Experimental Biomedicine, FZ 82) to H.S. We would like to thank Dr. Jochen Kuper Christin Schäfer and Johannes Schiebel for help with data collection.

Received: February 16, 2011
Revised: March 19, 2011
Accepted: March 22, 2011
Published: June 7, 2011

REFERENCES

Adams, P.D., Afonine, P.V., Bunkoczi, G., Chen, V.B., Davis, I.W., Echols, N., Headd, J.J., Hung, L.W., Kapral, G.J., Grosse-Kunstleve, R.W., et al. (2010). PHENIX: a comprehensive Python-based system for macromolecular structure solution. Acta Crystallogr. D Biol. Crystallogr. *66*, 213–221.

Alexandru, G., Graumann, J., Smith, G.T., Kolawa, N.J., Fang, R., and Deshaies, R.J. (2008). UBXD7 binds multiple ubiquitin ligases and implicates p97 in HIF1alpha turnover. Cell *134*, 804–816.

Beuron, F., Dreveny, I., Yuan, X., Pye, V.E., McKeown, C., Briggs, L.C., Cliff, M.J., Kaneko, Y., Wallis, R., Isaacson, R.L., et al. (2006). Conformational changes in the AAA ATPase p97-p47 adaptor complex. EMBO J. *25*, 1967–1976.

Bruderer, R.M., Brasseur, C., and Meyer, H.H. (2004). The AAA ATPase p97/VCP interacts with its alternative co-factors, Ufd1-Npl4 and p47, through a common bipartite binding mechanism. J. Biol. Chem. *279*, 49609–49616.

Buchberger, A., Howard, M.J., Proctor, M., and Bycroft, M. (2001). The UBX domain: a widespread ubiquitin-like module. J. Mol. Biol. *307*, 17–24.

Carim-Todd, L., Escarceller, M., Estivill, X., and Sumoy, L. (2001). Identification and characterization of UBXD1, a novel UBX domain-containing gene on human chromosome 19p13, and its mouse ortholog. Biochim. Biophys. Acta *1517*, 298–301.

CCP4 (Collaborative Computational Project, Number 4). (1994). The CCP4 suite—programs for protein crystallography. Acta Crystallogr. D Biol. Crystallogr. *50*, 760–763.

Davis, I.W., Leaver-Fay, A., Chen, V.B., Block, J.N., Kapral, G.J., Wang, X., Murray, L.W., Arendall, W.B., 3rd, Snoeyink, J., Richardson, J.S., et al. (2007). MolProbity: all-atom contacts and structure validation for proteins and nucleic acids. Nucleic Acids Res. *35*, W375–W383.

DeLaBarre, B., and Brunger, A.T. (2003). Complete structure of p97/valosin-containing protein reveals communication between nucleotide domains. Nat. Struct. Biol. *10*, 856–863.

Dikic, I., Wakatsuki, S., and Walters, K.J. (2009). Ubiquitin-binding domains—from structures to functions. Nat. Rev. Mol. Cell Biol. *10*, 659–671.

Dreveny, I., Kondo, H., Uchiyama, K., Shaw, A., Zhang, X., and Freemont, P.S. (2004). Structural basis of the interaction between the AAA ATPase p97/VCP and its adaptor protein p47. EMBO J. *23*, 1030–1039.

Emsley, P., and Cowtan, K. (2004). Coot: model-building tools for molecular graphics. Acta Crystallogr. D Biol. Crystallogr. *60*, 2126–2132.

Evans, P. (2006). Scaling and assessment of data quality. Acta Crystallogr. D Biol. Crystallogr. *62*, 72–82.

Gouet, P., Courcelle, E., Stuart, D.I., and Metoz, F. (1999). ESPript: analysis of multiple sequence alignments in PostScript. Bioinformatics *15*, 305–308.

Haines, D.S. (2010). p97-containing complexes in proliferation control and cancer: emerging culprits or guilt by association? Genes Cancer *1*, 753–763.

Halawani, D., and Latterich, M. (2006). p97: the cell's molecular purgatory? Mol. Cell *22*, 713–717.

Hänzelmann, P., Stingele, J., Hofmann, K., Schindelin, H., and Raasi, S. (2010). The yeast E4 ubiquitin ligase Ufd2 interacts with the ubiquitin-like domains of Rad23 and Dsk2 via a novel and distinct ubiquitin-like binding domain. J. Biol. Chem. *285*, 20390–20398.

Hirsch, C., Gauss, R., Horn, S.C., Neuber, O., and Sommer, T. (2009). The ubiquitylation machinery of the endoplasmic reticulum. Nature *458*, 453–460.

Holm, L., Kaariainen, S., Rosenstrom, P., and Schenkel, A. (2008). Searching protein structure databases with DaliLite v.3. Bioinformatics *24*, 2780–2781.

Isaacson, R.L., Pye, V.E., Simpson, P., Meyer, H.H., Zhang, X., Freemont, P.S., and Matthews, S. (2007). Detailed structural insights into the p97-Npl4-Ufd1 interface. J. Biol. Chem. *282*, 21361–21369.

Johnson, J.O., Mandrioli, J., Benatar, M., Abramzon, Y., Van Deerlin, V.M., Trojanowski, J.Q., Gibbs, J.R., Brunetti, M., Gronka, S., Wuu, J., et al. (2010). Exome sequencing reveals VCP mutations as a cause of familial ALS. Neuron *68*, 857–864.

Ju, J.S., and Weihl, C.C. (2010). Inclusion body myopathy, Paget's disease of the bone and fronto-temporal dementia: a disorder of autophagy. Hum. Mol. Genet. *19*, R38–R45.

Kabsch, W., and Sander, C. (1983). Dictionary of protein secondary structure: pattern recognition of hydrogen-bonded and geometrical features. Biopolymers *22*, 2577–2637.

Kang, W., and Yang, J.K. (2011). Crystal structure of human FAF1 UBX domain reveals a novel FcisP touch-turn motif in p97/VCP-binding region. Biochem. Biophys. Res. Commun. *407*, 531–534.

Kern, M., Fernandez-Saiz, V., Schafer, Z., and Buchberger, A. (2009). UBXD1 binds p97 through two independent binding sites. Biochem. Biophys. Res. Commun. *380*, 303–307.

Leslie, A.G.W. (1992). Recent changes to the MOSFLM package for processing film and image plate data. Joint CCP4+ESF-EAMCB Newsletter on Protein Crystallography No. 26, pp. 27–33.

Madsen, L., Andersen, K.M., Prag, S., Moos, T., Semple, C.A., Seeger, M., and Hartmann-Petersen, R. (2008). Ubxd1 is a novel co-factor of the human p97 ATPase. Int. J. Biochem. Cell Biol. *40*, 2927–2942.

McCoy, A.J., Grosse-Kunstleve, R.W., Adams, P.D., Winn, M.D., Storoni, L.C., and Read, R.J. (2007). *Phaser* crystallographic software. J. Appl. Crystallogr. *40*, 658–674.

Menges, C.W., Altomare, D.A., and Testa, J.R. (2009). FAS-associated factor 1 (FAF1): diverse functions and implications for oncogenesis. Cell Cycle *8*, 2528–2534.

Meyer, H.H., Shorter, J.G., Seemann, J., Pappin, D., and Warren, G. (2000). A complex of mammalian ufd1 and npl4 links the AAA-ATPase, p97, to ubiquitin and nuclear transport pathways. EMBO J. *19*, 2181–2192.

Neuber, O., Jarosch, E., Volkwein, C., Walter, J., and Sommer, T. (2005). Ubx2 links the Cdc48 complex to ER-associated protein degradation. Nat. Cell Biol. *7*, 993–998.

Pye, V.E., Dreveny, I., Briggs, L.C., Sands, C., Beuron, F., Zhang, X., and Freemont, P.S. (2006). Going through the motions: the ATPase cycle of p97. J. Struct. Biol. *156*, 12–28.

Pye, V.E., Beuron, F., Keetch, C.A., McKeown, C., Robinson, C.V., Meyer, H.H., Zhang, X., and Freemont, P.S. (2007). Structural insights into the p97-Ufd1-Npl4 complex. Proc. Natl. Acad. Sci. USA *104*, 467–472.

Rape, M., Hoppe, T., Gorr, I., Kalocay, M., Richly, H., and Jentsch, S. (2001). Mobilization of processed, membrane-tethered SPT23 transcription factor by CDC48(UFD1/NPL4), a ubiquitin-selective chaperone. Cell *107*, 667–677.

Rouiller, I., Butel, V.M., Latterich, M., Milligan, R.A., and Wilson-Kubalek, E.M. (2000). A major conformational change in p97 AAA ATPase upon ATP binding. Mol. Cell *6*, 1485–1490.

Schuberth, C., and Buchberger, A. (2005). Membrane-bound Ubx2 recruits Cdc48 to ubiquitin ligases and their substrates to ensure efficient ER-associated protein degradation. Nat. Cell Biol. *7*, 999–1006.

Schuberth, C., and Buchberger, A. (2008). UBX domain proteins: major regulators of the AAA ATPase Cdc48/p97. Cell. Mol. Life Sci. *65*, 2360–2371.

Song, E.J., Yim, S.H., Kim, E., Kim, N.S., and Lee, K.J. (2005). Human Fas-associated factor 1, interacting with ubiquitinated proteins and valosin-containing protein, is involved in the ubiquitin-proteasome pathway. Mol. Cell. Biol. *25*, 2511–2524.

Tang, W.K., Li, D., Li, C.C., Esser, L., Dai, R., Guo, L., and Xia, D. (2010). A novel ATP-dependent conformation in p97 N-D1 fragment revealed by crystal structures of disease-related mutants. EMBO J. *29*, 2217–2229.

Vij, N. (2008). AAA ATPase p97/VCP: cellular functions, disease and therapeutic potential. J. Cell. Mol. Med. *12*, 2511–2518.

Ye, Y. (2006). Diverse functions with a common regulator: ubiquitin takes command of an AAA ATPase. J. Struct. Biol. *156*, 29–40.

Yeung, H.O., Kloppsteck, P., Niwa, H., Isaacson, R.L., Matthews, S., Zhang, X., and Freemont, P.S. (2008). Insights into adaptor binding to the AAA protein p97. Biochem. Soc. Trans. *36*, 62–67.

Zhang, X., Shaw, A., Bates, P.A., Newman, R.H., Gowen, B., Orlova, E., Gorman, M.A., Kondo, H., Dokurno, P., Lally, J., et al. (2000). Structure of the AAA ATPase p97. Mol. Cell *6*, 1473–1484.